Supporting Information

Silicon Atom Doping in Heterotrimetallic Sulfides for Non-noble Metal Alkaline Water Electrolysis

Mohamed Barakat Zakaria Hegazy,[1,2*] Leila Bahri,[3] David Tetzlaff,[1,4] Sebastian Sanden,[1] Ulf-Peter Apfel[1,4*]

1. *Inorganic Chemistry I – Technical Electrochemistry, Faculty for Chemistry and Biochemistry, Ruhr University Bochum, 44801 Bochum, Germany,*
2. *Department of Chemistry, Faculty of Science, Tanta University, 31527 Tanta, Egypt,*
3. *Department of Chemistry, College of Sciences, University of Hafar Al-Batin, 39524 Hafar Al-Batin, Kingdom of Saudi Arabia.*
4. *Fraunhofer Institute for Environmental, Department for Electrosynthesis, Safety and Energy Technology UMSICHT, 46047 Oberhausen, Germany*

mohamed.barakat@rub.de and ulf.apfel@rub.de

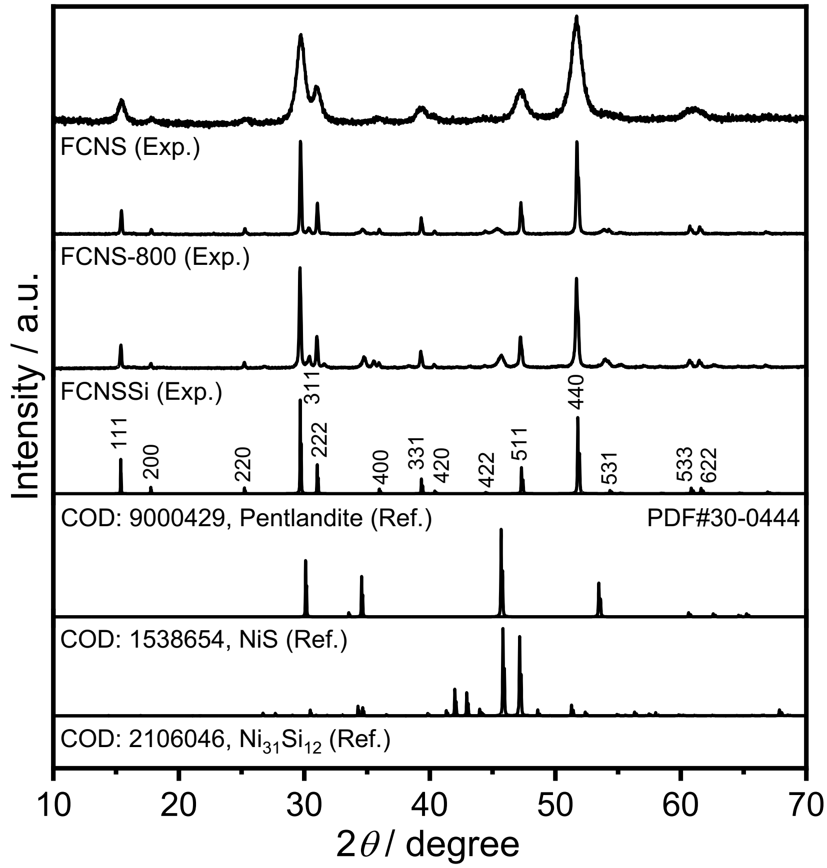

Figure S1 Phase analysis of the PXRD patterns collected on FCNS, FCNS-800, and FCNSSi powders.

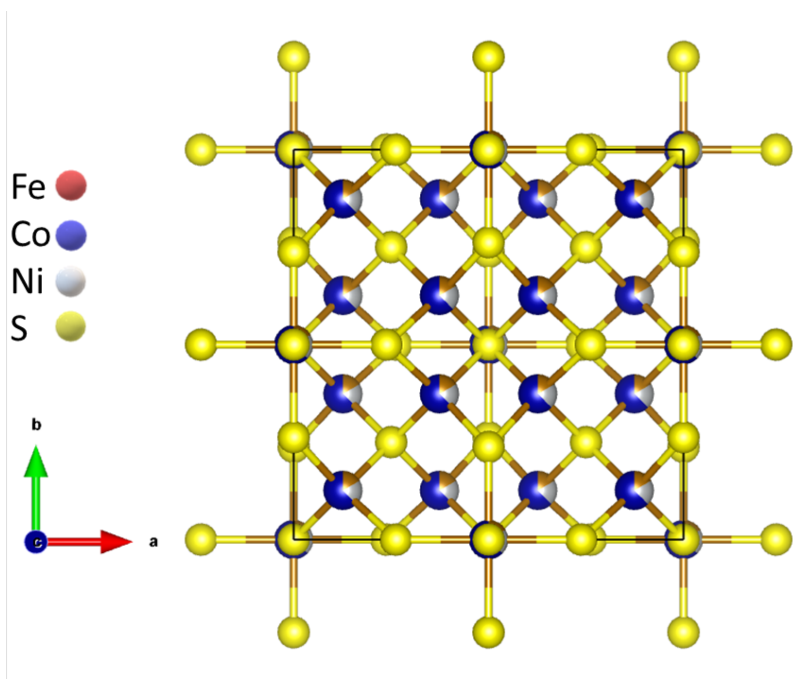

Figure S2 Crystal structure illustration of trimetallic (Fe, Co, Ni) pentlandite-phase (PDF#30-0444).

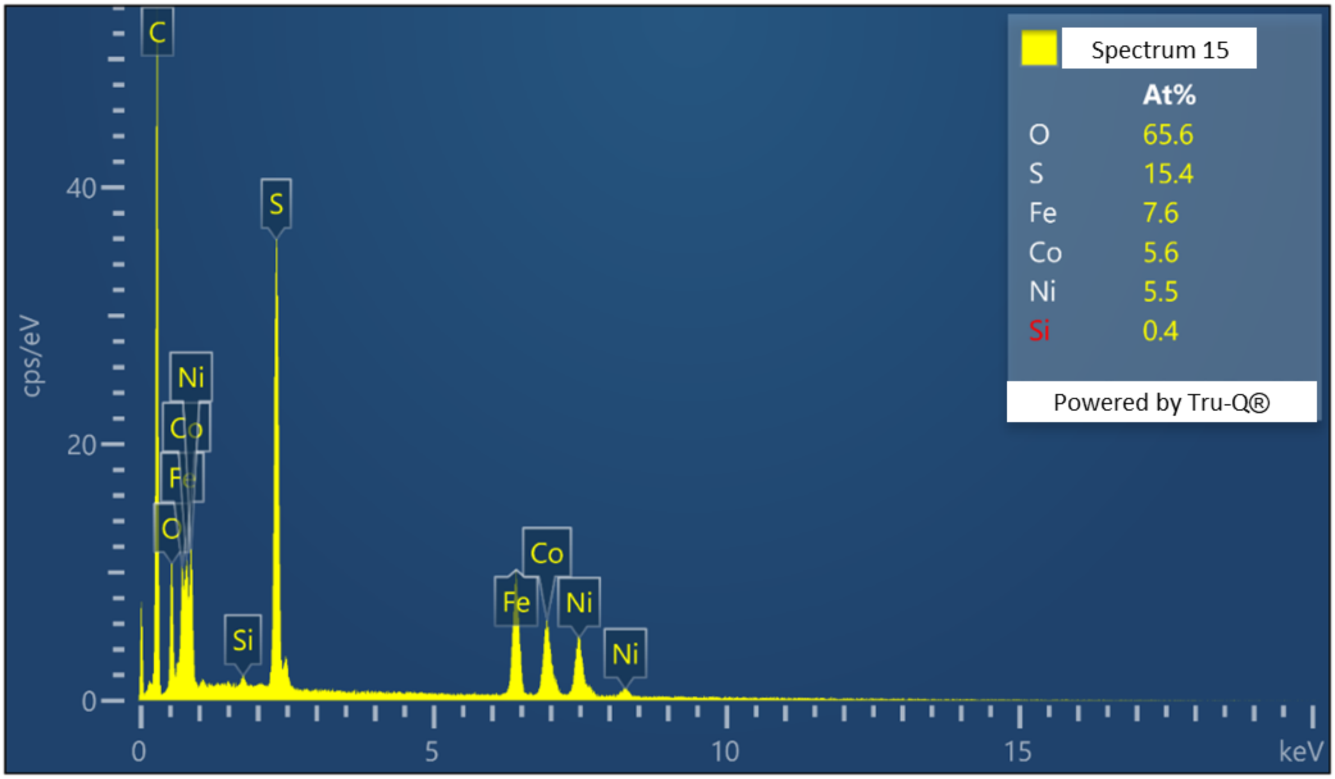

Figure S3 EDX spectra of the as-prepared FCNSSi powder.

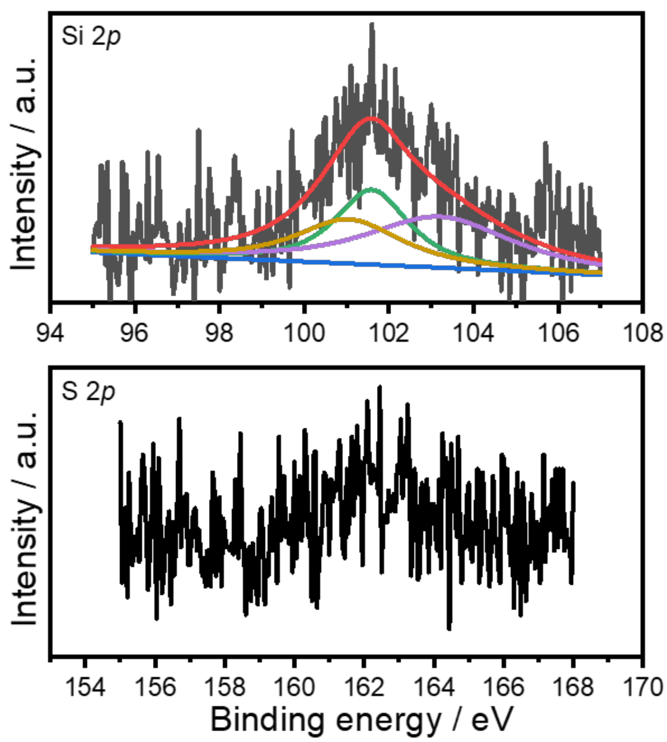

Figure S4 High-resolution XPS spectra of S 2*p*, and Si 2*p* orbitals collected from wide scan survey of FCNSSi-RT sample.

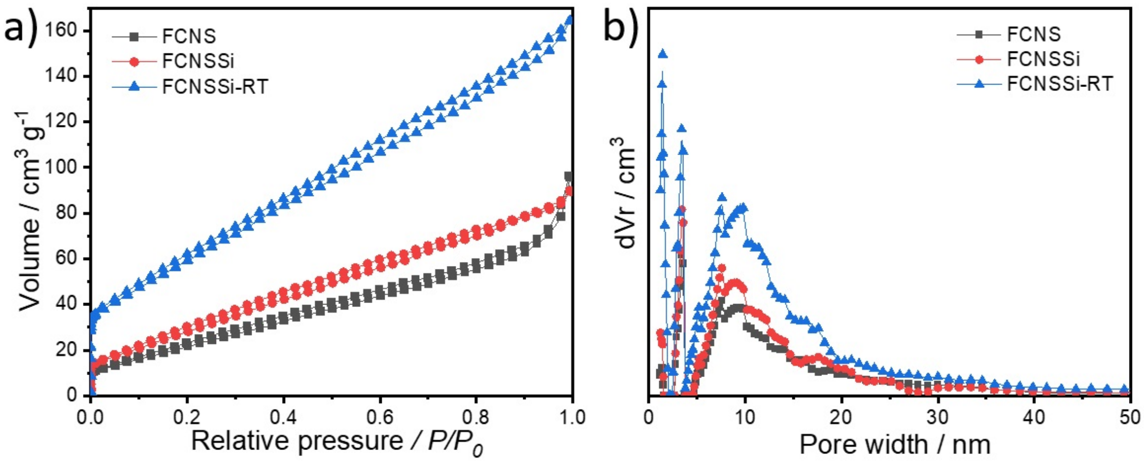

Figure S5 a) Nitrogen gas sorption isotherms, and b) average pore size distribution curves of FCNS, FCNSSi, and FCNSSi-RT powders.

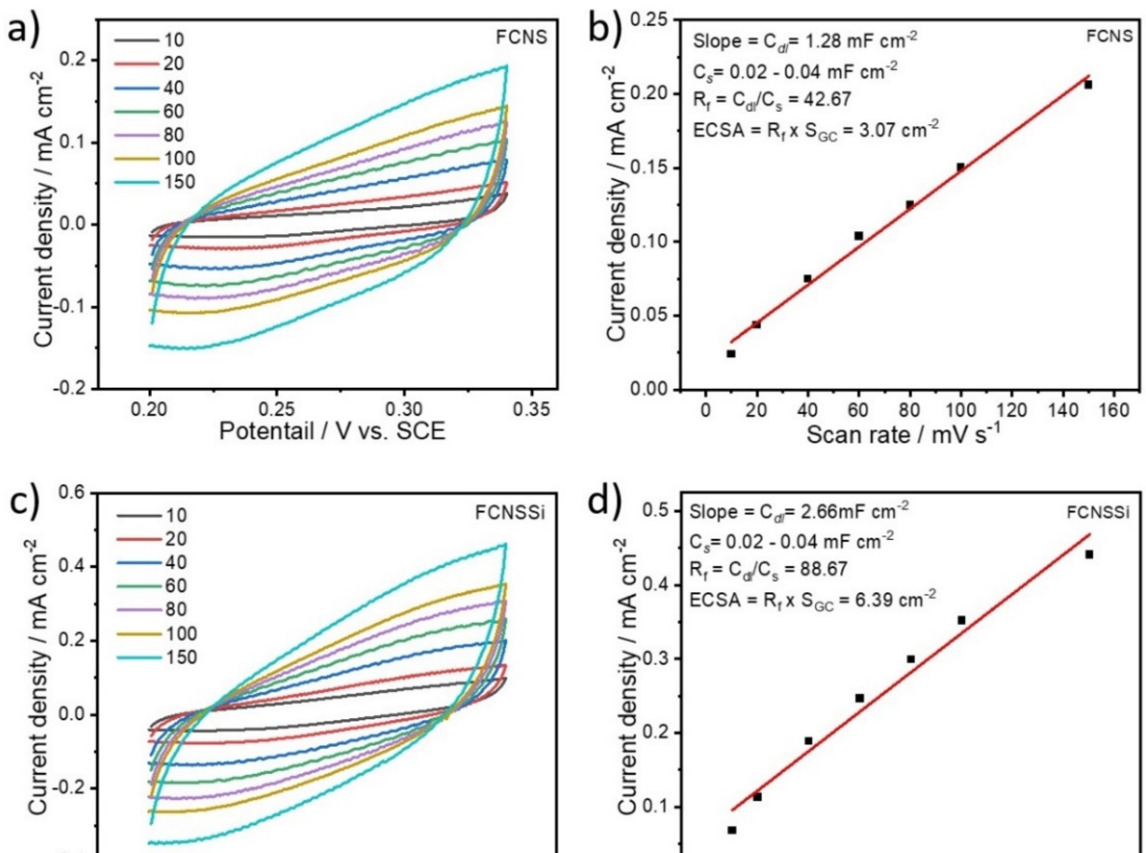

Figure S6 CV curves a,c) at 10, 20, 40, 60, 80, 100, and 150 mV s^{-1} in 1.0 M KOH solution and b,d) double layer charging current *vs.* scan rate plots of pristine FCNS and doped FCNSSi on classy carbon electrode to determine ECSA.

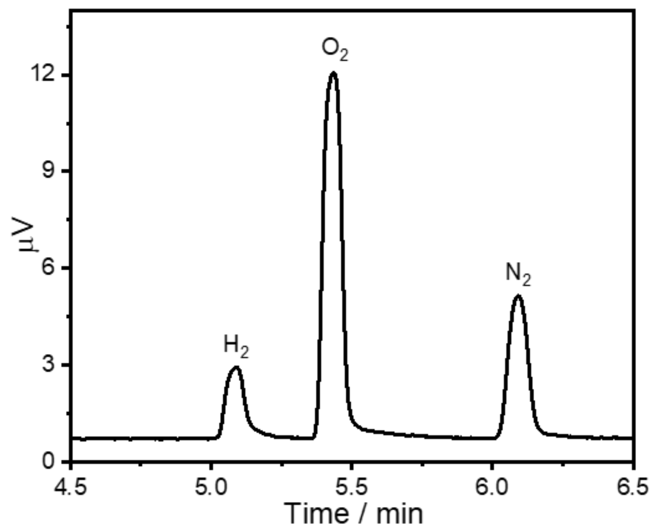

Figure S7 Gas chromatograms (GC) of oxygen determination during# 1h of OER performance at 20 mA cm^{-2}.

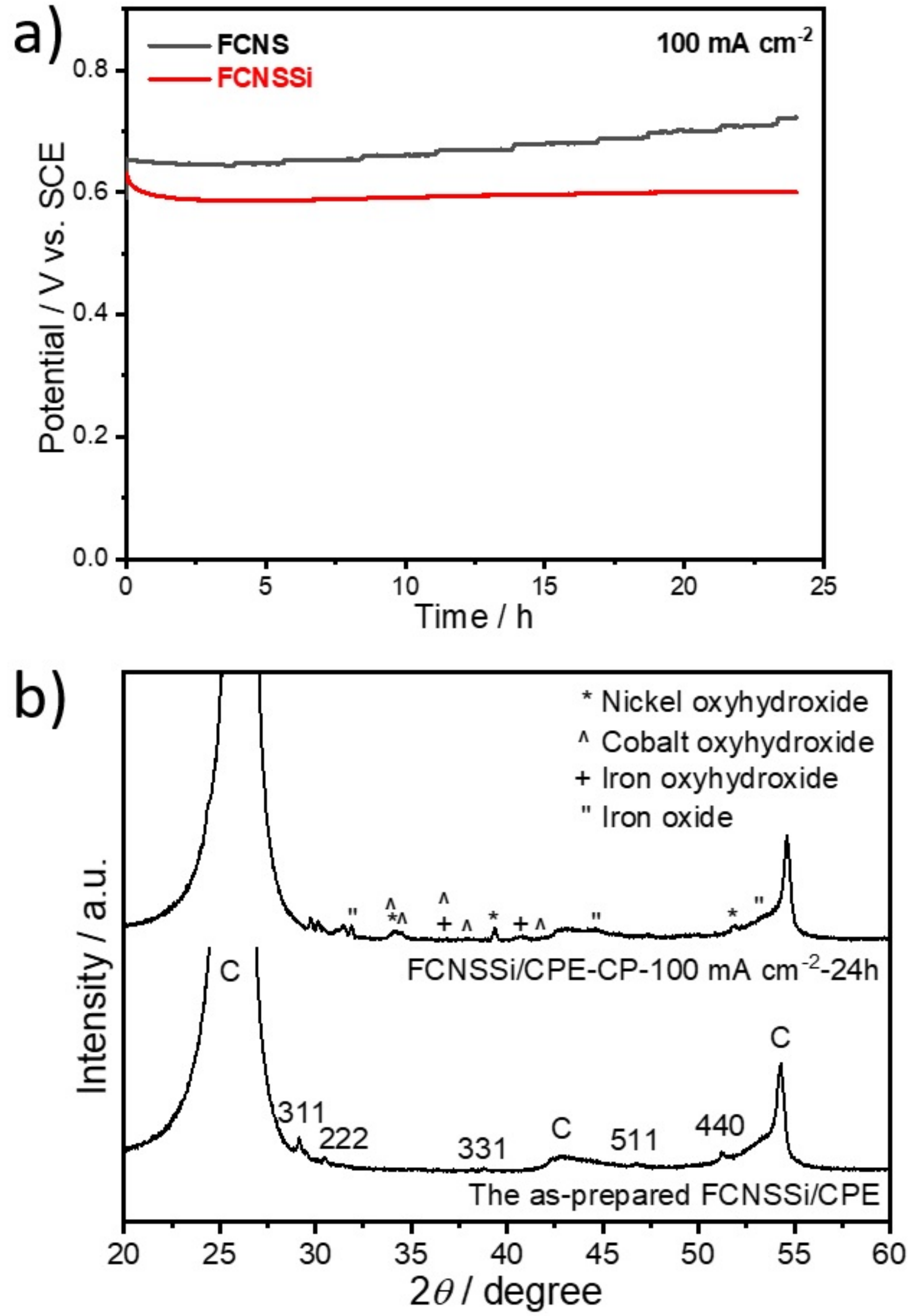

Figure S8 a) Chronopotentiometry measurements of our materials on carbon paper electrode at 100 mA cm^{-2} for 24h, and b) PXRD patterns of FCNSS/CE before and after chronopotentiometry test at 100 mA cm^{-2} for 24h.

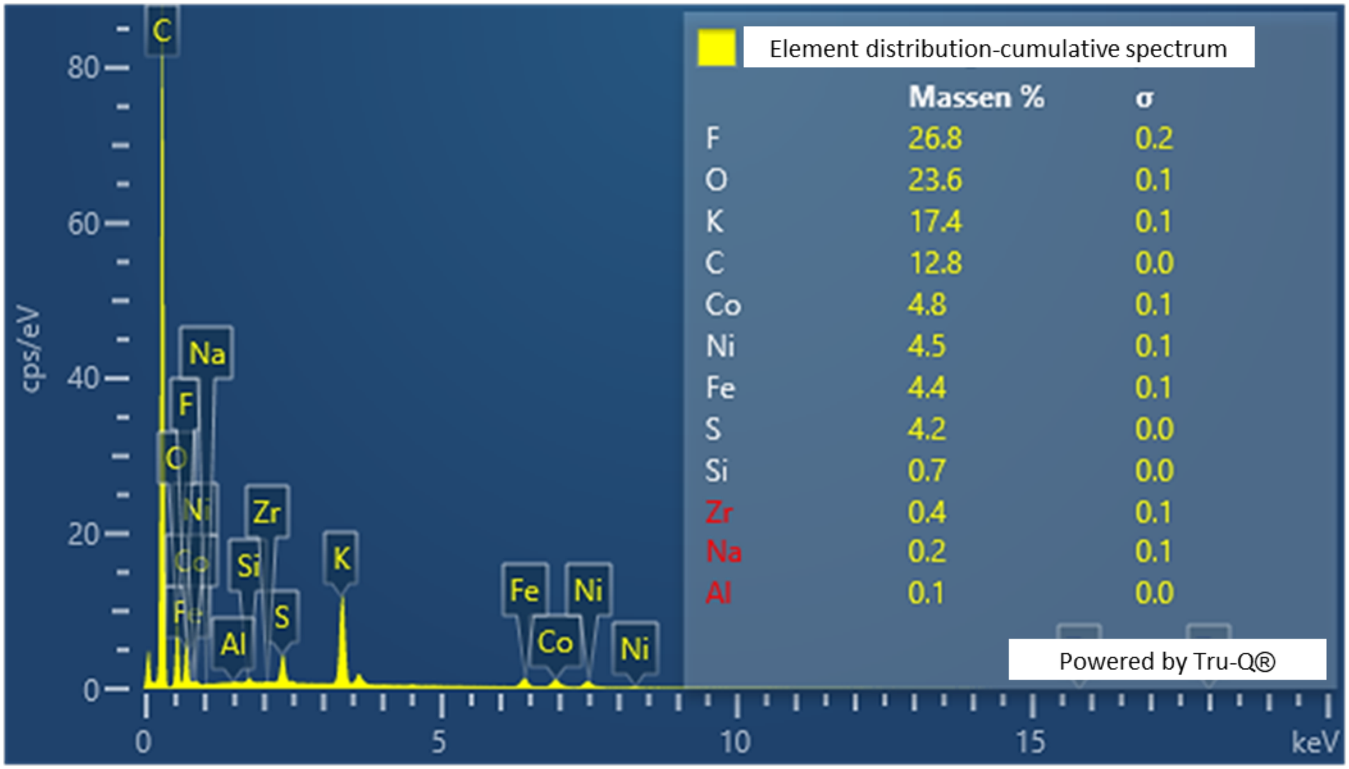

Figure S9 EDX spectra of the FCNSSi sample on carbon paper electrode after chronopotentiometry test at 100 mA cm^{-2} for 24h.

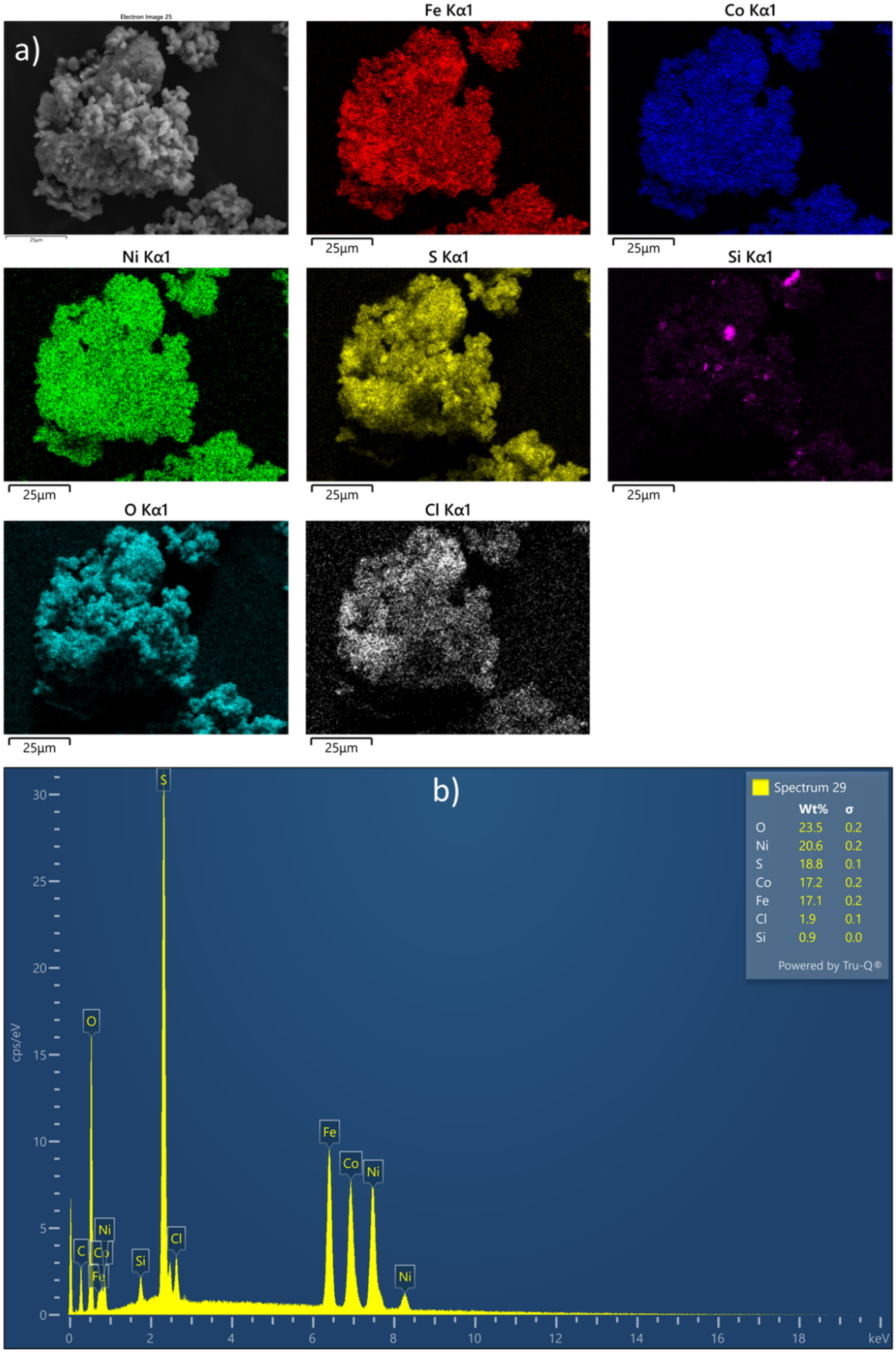

Figure S10 a) SEM image and the corresponding atoms mapping (Fe, Co, Ni, S, Si, O, and Cl), and b) EDX spectra of FCNSSi-RT powder sample.

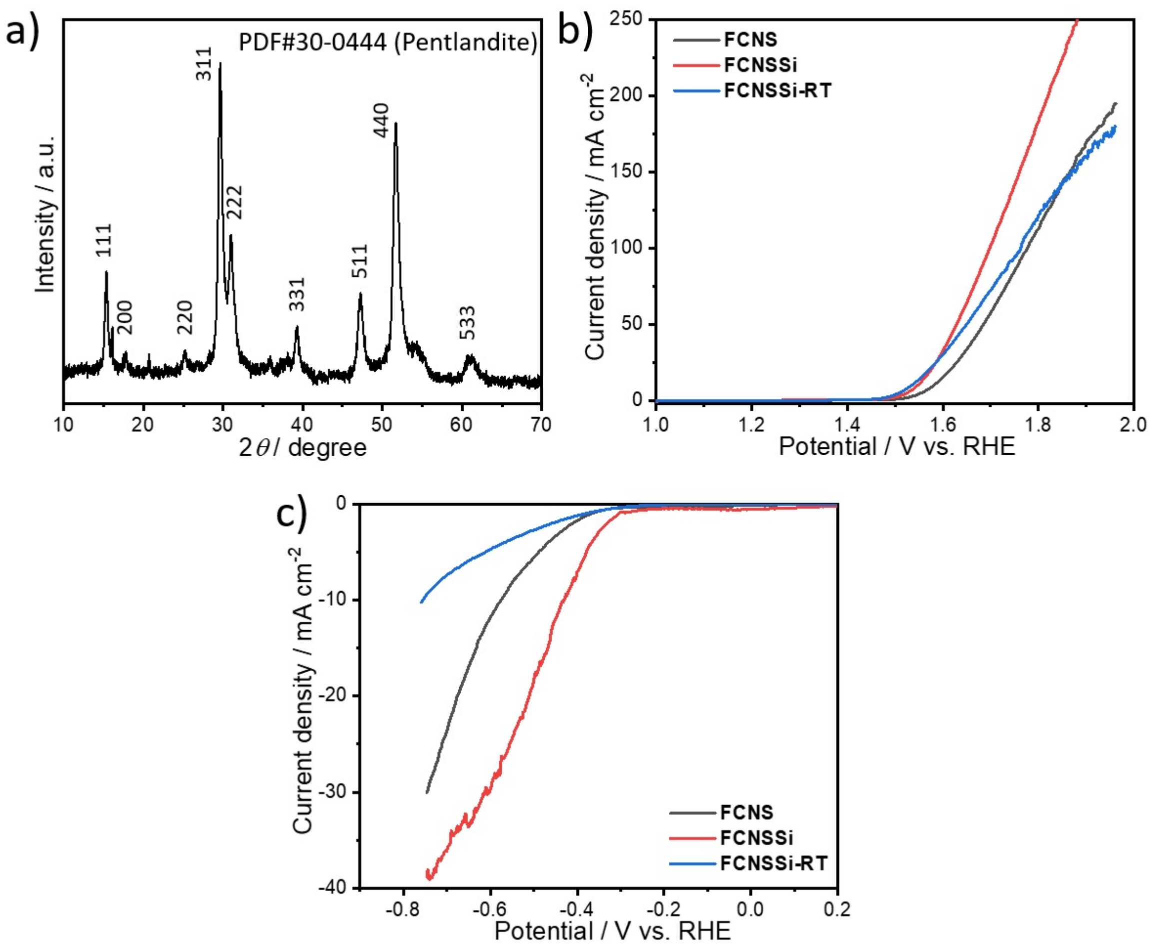

Figure S11 a) PXRD pattern of FCNSSi-RT powder and LSV curves in b) 1.0 M KOH and c) 0.5 M H_2SO_4 of FCNSS-RT sample at a scan rate of 50.0 mV s^{-1} on glassy carbon electrode (GCE).

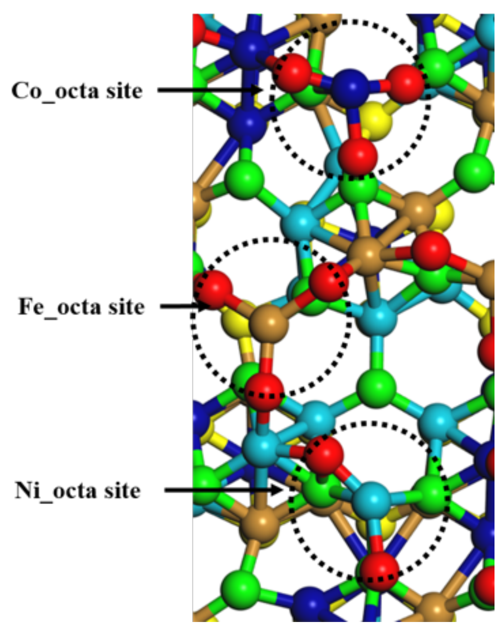

Figure S12 Top view of optimized the metal octahedral site (Fe, Co and Ni) in FCNSSi surface covered with 7/4 O* ML.

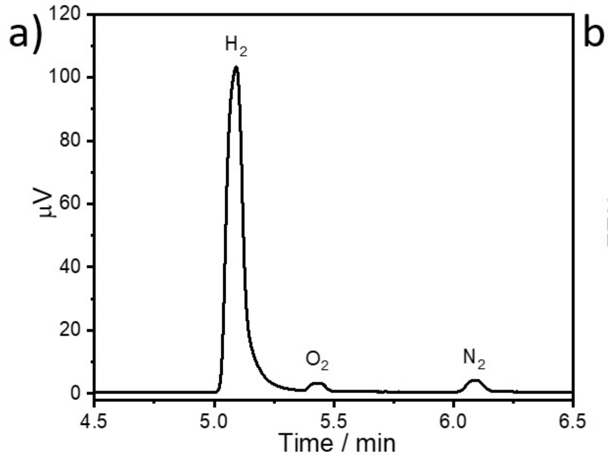

Figure S13 Gas chromatograms for hydrogen determination during 1h of HER performance at -20 mA cm^{-2}, and b) the calculated faradic efficiency percentage (FE%).

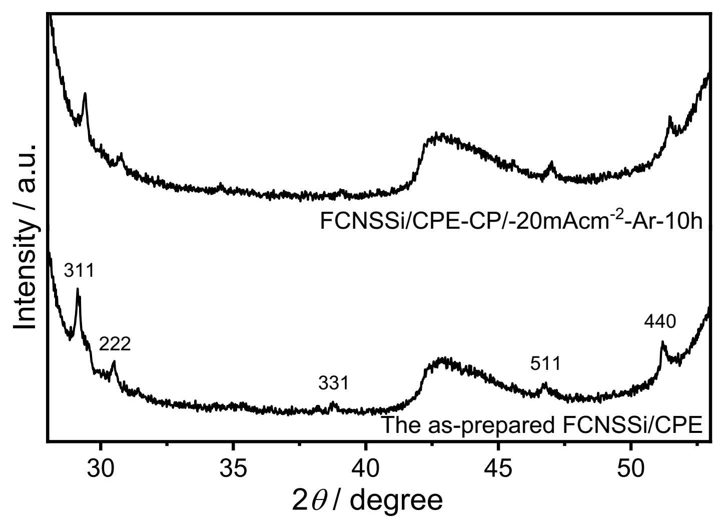

Figure S14 PXRD of FCNSSi/CE before and after chronopotentiometry test at -20 mA cm^{-2} for 10 h in argon.

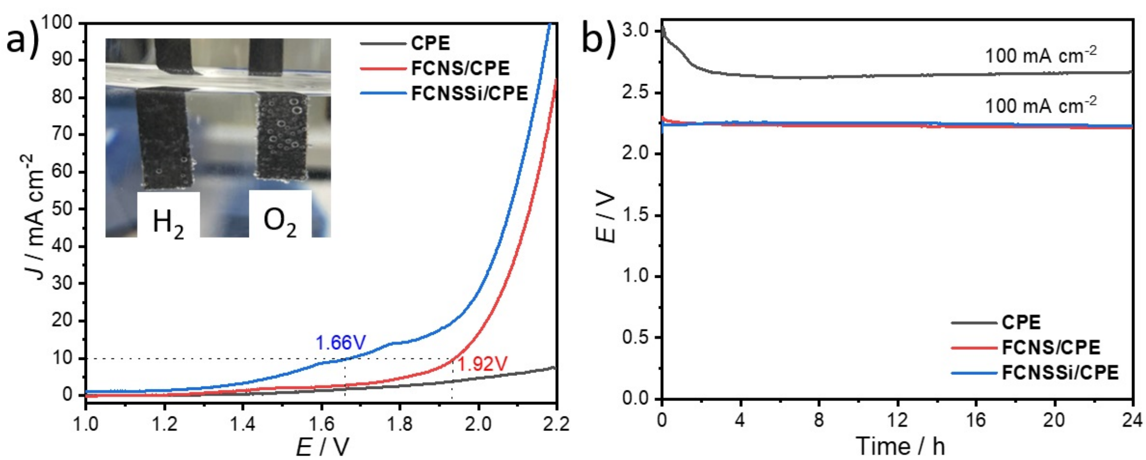

Figure S15 a) LSV curves for the overall water splitting using FCNS and FCNSSi at both cathode and anode at a scan rate of 10 mV s^{-1} in 1.0 M KOH solution. b) Chronopotentiometry test of bare CPE, pristine FCNS, and FCNSSi electrodes at 100 mA cm^{-2}.

The overall electrochemical water spitting test on FCNSSi

The results presented here clearly demonstrate that the FCNSSi electrode is a highly active and stable bifunctional electrocatalyst for both oxygen evolution reaction (OER) and hydrogen evolution reaction (HER). To investigate its potential for overall water splitting, we designed a two-electrode cell in which FCNSSi served as both anode and cathode in an alkaline solution (see inset in **Figure S15a**). The FCNSSi electrode showed impressive activity, achieving a water-splitting current density of 10 mA cm^{-2} at a potential of 1.66 V. This represents a significant reduction in overpotential of 260 mV compared to the pristine FCNS electrode (1.92 V), and is comparable to previously reported non-noble bifunctional electrocatalysts for water splitting [1].

Furthermore, a chronopotentiometry test conducted at 100 mA cm^{-2} for 24 hours confirmed the high stability of the FCNSSi electrode with an overall cell potential of 2.19 V, indicating its potential for practical application in overall water splitting in an alkaline environment (**Figure S15b**).

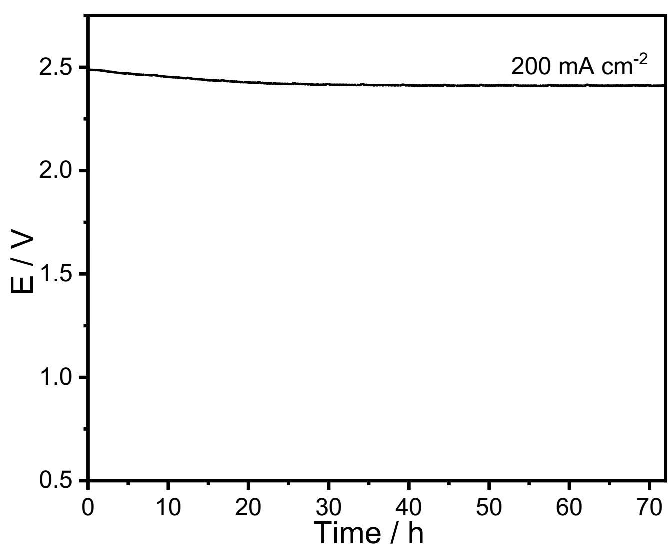

Figure S16 Chronopotentiometry test of FCNSSi/CPE at 200 mA cm^{-2} in 1.0M KOH for three executive days.

Remarkably, the FCNSSi electrode exhibited efficient and stable water-splitting performance for three consecutive days at 200 mA cm^{-2}, with a decrease in the overall cell potential from 2.49 V to 2.41 V (**Figure S16**). Overall, these findings demonstrate the promising potential of the FCNSSi electrode as an efficient and stable electrocatalyst for overall water splitting in alkaline solutions, making it a strong candidate for practical application in various renewable energy conversion and storage systems.

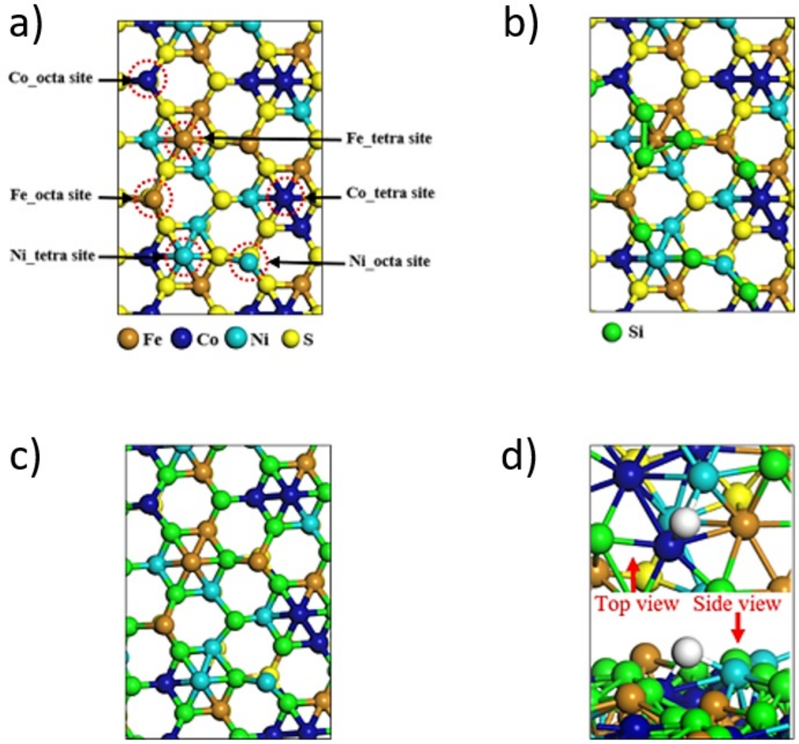

Figure S17 a) Top view of optimized (111) pristine FCNS surface, b) Top view of optimized (111) Si adsorbed on FCNS surface (FCNSSi-RT), c) Top view of optimized (111) FCNS surface doped Si (FCNSSi), d) Top view and side view of hydrogen adsorption on FCNSSi.

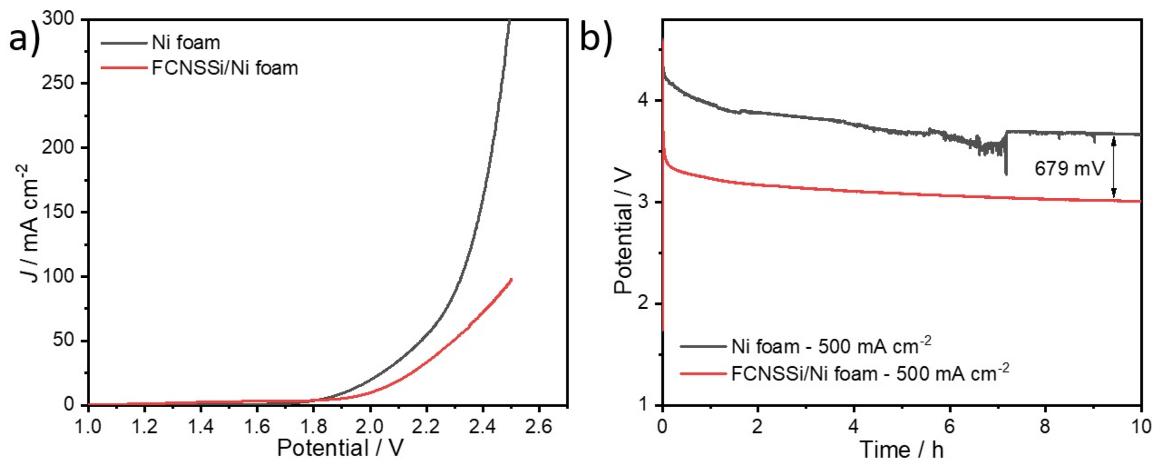

Figure S18 a) LSV curves and b) chronopotentiometry test at 500 mA cm^{-2} for 10 h collected using zero-gap cell in 1.0M KOH and using a FumaSep AEM.

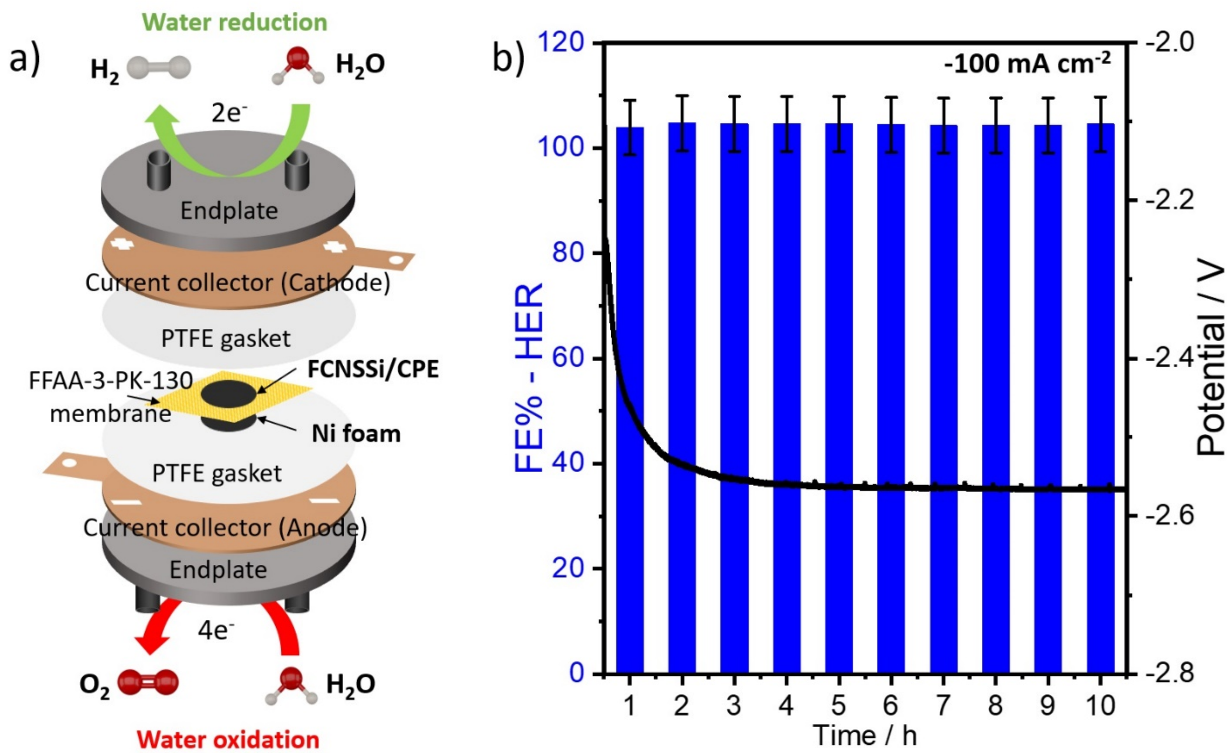

Figure S19 a) Zero-gap cell assembly using FCNSSi on CPE at cathodic side against Ni foam at anodic side, and b) chronopotentiometry test at -100 mA cm^{-2} for 10 h and the estimated FE% for HER.

Table S1 Atomic percentage of elements in our materials determined by ICP-OES analysis.

Sample name	*%Fe*	*%Co*	*%Ni*	*%S*	*%Si*
FCNSSi	18.61	19.11	19.21	30.68	0.91
FCNSSi-RT	16.23	16.51	16.52	26.24	5.74

Table S2 OER performance of our materials against the previously reported pentlandites electrocatalysts.

Sample name	*J/mA cm^{-2}*	*η/mV*	*Tafel slope/mV dec^{-1}*	*Electrolyte*	*Electrode*	*Reference*
FCNSSi	10	316	70	1.0MKOH	GCE	This study
FCNSP	10	419	76	1.0MKOH	GCE	[S1]
FCNSN	10	390	64	1.0MKOH	GCE	[S1]
FCNSNP	10	349	51	1.0MKOH	GCE	[S1]
FCNSP	100	479	51	1.0MKOH	CPE	[S1]
FCNSN	100	440	70	1.0MKOH	CPE	[S1]
FCNSNP	100	427	46	1.0MKOH	CPE	[S1]
Ni_9S_8	10	354	56	1.0MKOH	GCE	[S2]
$FeNi_8S_8$	10	371	55	1.0MKOH	GCE	[S2]
$Fe_2Ni_7S_8$	10	359	55	1.0MKOH	GCE	[S2]
$Fe_3Ni_6S_8$	10	367	61	1.0MKOH	GCE	[S2]
$Fe_4Ni_5S_8$	10	386	56	1.0MKOH	GCE	[S2]
$Fe_5Ni_4S_8$	10	401	60	1.0MKOH	GCE	[S2]
$Fe_6Ni_3S_8$	10	423	75	1.0MKOH	GCE	[S2]
$Fe_7Ni_2S_8$	10	434	91	1.0MKOH	GCE	[S2]
Fe_8NiS_8	10	495	75	1.0MKOH	GCE	[S2]
Fe_9S_8	---	---	168	1.0MKOH	GCE	[S2]
Co_9S_8 spheres	10	285	58	1.0MKOH	GCE	[S3]
Co_9S_8 flowers	10	380	76	1.0MKOH	GCE	[S3]
NSC/$Ni_4Fe_5S_8$-1000	10	620	431	1.0MKOH	GCE	[S4]

PNSC/$Ni_4Fe_5S_8$-1000	10	300	72	0.5MH_2SO_4	GCE	[S4]
PNSC/$Ni_4Fe_5S_8$-1000	10	280	---	1.0MKOH	GCE	[S4]
$Ni_{4.3}Co_{4.7}S_8$	20	133	194	1.0MKOH	Ni foam	[S5]
Co_9S_8/CNS	10	294	50.1	1.0MKOH	RDE	[S6]
Co_9S_8	10	340	85.6	1.0MKOH	RDE	[S6]

Table S3 HER performance of our materials against the previously reported pentlandites electrocatalysts.

Sample name	*J/mA cm^{-2}*	*η/mV*	*Tafel slope/mV dec^{-1}*	*Electrolyte*	*Electrode*	*Reference*
FCNSSi	10	164	80.7	0.5MH_2SO_4	GCE	This study
FCNSP	10	473	133	0.5MH_2SO_4	GCE	[S1]
FCNSN	10	344	164	0.5MH_2SO_4	GCE	[S1]
$Ni_{4.3}Co_{4.7}S_8$	10	148	90.0	1.0MKOH	Ni foam	[S5]
Ni foam	100	238.0	175.5	1.0MKOH	Ni foam	[S5]
CoS	10	174.2	157.7	1.0MKOH	Ni foam	[S5]
$Ni_{0.1}Co_{0.9}S$	10	174.2	157.7	1.0MKOH	Ni foam	[S5]
$Ni_{1.4}Co_{7.6}S_8$	10	196.6	156.9	1.0MKOH	Ni foam	[S5]
Ni3S2	10	209.8	135.5	1.0MKOH	Ni foam	[S5]
Ni4.5Fe4.5S8	10	280		0.5 M H_2SO_4	Rocks	[S7]
$Fe_{4.5}Ni_{4.5}S_8$	10	190	76	0.5 M H_2SO_4	Pellet	[S8]
$Fe_{4.5}Ni_{4.5}S_7Se_1$	10	172	120	0.5 M H_2SO_4	Pellet	[S8]
$Fe_{4.5}Ni_{4.5}S_6$Se2	10	230	120	0.5 M H_2SO_4	Pellet	[S8]
Ni@NC-800	10	205	160	1.0 M KOH	Ni foam	[S9]
Co_9S_8@MoS_2/CNFs	10	190	110	1.0 M KOH	CNFs	[S10]
Ni/Ni_3C/C-NCNT	10	184	98.7	1.0 M KOH	GCE	[S11]
N-doped NiMoS	10	68.0	86.0	1.0 M KOH	Ni foam	[S12]
Ni_3S_2	10	335	97.0	1.0 M KOH	GCE	[S13]
NiS_2	10	454	124	1.0 M KOH	GCE	[S13]
NiS	10	474	128	1.0 M KOH	GCE	[S13]
Co_9S_8-60	10	178	82.0	0.5 M H2SO4	GCE	[S14]
Nanoporous-Co_9S_8	10	264	118	1.0 M PBS	RDE	[S15]
Porous-$Co_9S_4P_4$/Fe	10	87.0	51.0	1.0 M PBS	RDE	[S15]
MoS_2/$CoMo_2S_4$	10	122	90.0	1.0 M KOH	GCE	[S16]
Ni/NiS/P,N,S-rGO	10	155	135	1.0 M KOH	CPE	[S17]

Table S4 FE% of our materials against the previously reported pentlandites electrocatalysts for HER.

Sample name	FE%	Time/h	*Electrolyte*	*Electrode*	*Reference*
FCNSSi	109$\pm$10	10.0	0.5 M H_2SO_4	CPE	This study
FCNS	95.4$\pm$2	10.0	0.5 M H_2SO_4	CPE	[S1]
FCNSN	98.1$\pm$2	10.0	0.5 M H_2SO_4	CPE	[S1]
FCNSNP	97.5$\pm$2	10.0	0.5 M H_2SO_4	CPE	[S1]
$Ni_{4.5}Fe_{4.5}S_8$	91.0$\pm$5	5.0	0.5 M H_2SO_4	Rocks	[S7]
$Fe_{4.5}Ni_{4.5}S_8$	90.2$\pm$5	4.0	0.5 M H_2SO_4	Pellet	[S8]
$Fe_{4.5}Ni_{4.7}S_7Se_1$	94.1$\pm$5	4.0	0.5 M H_2SO_4	Pellet	[S8]
$Fe_{4.5}Ni_{4.7}S_6Se_2$	98.5$\pm$5	4.0	0.5 M H_2SO_4	Pellet	[S8]
$Fe_{4.5}Ni_{4.7}S_5Se_3$	97.8$\pm$5	4.0	0.5 M H_2SO_4	Pellet	[S8]
$Fe_{4.5}Ni_{4.7}S_4Se_4$	95.9$\pm$5	4.0	0.5 M H_2SO_4	Pellet	[S8]
$Fe_{4.5}Ni_{4.7}S_3Se_5$	96.7$\pm$5	4.0	0.5 M H_2SO_4	Pellet	[S8]

References

[S1] M. B. Z. Hegazy, K. Harrath, D. Tetzlaff, M. Smialkowski, D. Siegmund, J. Li, R. Cao, U.-P. Apfel, *iScience* **2022**, *25*, 105148.

[S2] H. M. A. Amin, M. Attia, D. Tetzlaff, U.-P. Apfel, *ChemElectroChem* **2021**, *8*, 3863–3874.

[S3] X. Feng, Q. Jiao, T. Liu, Q. Li, M. Yin, Y. Zhao, H. Li, C. Feng, W. Zhou, *ACS Sustainable Chem. Eng.* **2018**, *6*, 1863–1871.
[S4] Q. Hu, G. Li, X. Liu, B. Zhu, G. Li, L. Fan, X. Chai, Q. Zhang, J. Liu, C. He, *J. Mater. Chem. A* **2019**, *7*, 461–468.
[S5] Y. Tang, H. Yang, J. Sun, M. Xia, W. Guo, L. Yu, J. Yan, J. Zheng, L. Chang, F. Gao, Nanoscale 2018, 10, 10459–10466.
[S6] M. Al-Mamun, Y. Wang, P. Liu, Y. L. Zhong, H. Yin, X. Su, H. Zhang, H. Yang, D. Wang, Z. Tang, H. Zhao, *J. Mater. Chem. A* **2016**, *4*, 18314-18321.
[S7] B. Konkena, K. Puring, I. Sinev, S. Piontek, O. Khavryuchenko, J. P. Dürholt, R. Schmid, H. Tüysüz, M. Muhler, W. Schuhmann, U.-P. Apfel, *Nat. Commun*. **2016**, 7, 12269.
[S8] M. Smialkowski, D. Siegmund, K. Pellumbi, L. Hensgen, H. Antoni, M. Muhler, U.-P. Apfel, *Chem. Commun*. **2019**, *55*, 8792–8795.
[S9] Y. Xu, W. Tu, B. Zhang, S. Yin, Y. Huang, M. Kraft, R. Xu, *Adv. Mater.* **2017**, *29*, 1605957.
[S10] H. Zhu, J. Zhang, R. Yanzhang, M. Du, Q. Wang, G. Gao, J. Wu, G. Wu, M. Zhang, B. Liu, J. Yao, X. Zhang, Adv. *Mater.* **2015**, *27*, 4752–4759.
[S11] T. Dong, X. Zhang, Z. Cao, H.-S. Chen, P. Yang,. *Inorg. Chem. Front.* **2019**, *6*, 1073–1080.
[S12] C. Huang, L. Yu, W. Zhang, Q. Xiao, J Zhou, Y. Zhang, P. An, J. Zhang, Y. Yu, *Appl. Catal. B Environ.* **2020**, *276*, 119137.
[S13] N. Jiang, Q. Tang, M. Sheng, B. You, D Jiang, Y. Sun, *Catal. Sci. Technol.* **2016**, *6*, 1077-1084.
[S14] Y. Yang, M. Yuan, H. Li, G. Sun, S. Ma, *Electrochim. Acta* **2018**, *281*, 198-207.
[S15] Y. Tan, M. Luo, P. Liu, C. Cheng, J. Han, K. Watanabe, M. Chen, *ACS Appl. Mater. Interfaces* **2019**, *11*, 3880–3888.
[S16] Y. Guo, J. Tang, J. Henzie, B. Jiang, W. Xia, T. Chen, Y. Bando, Y.-M. Kang, *ACS Nano* **2020**, *14*, 4141–4152.
[S17] M. B. Z. Hegazy, M. R. Berber, Y. Yamauchi, A. Pakdel, R. Cao,U. P. Apfel, *ACS Appl. Mater. Interfaces* **2021**, *13*, 34043-34052.